FIKUT NEXTGEN – MEETING OF YOUNG ASTRONOMERS AND ASTROPHYSICISTS

Early inspiral higher harmonics and Einstein Telescope geometry

Kata Karácsonyi

HUN-REN Wigner Research Centre for Physics
University of Szeged

06. November 2026

Gravitational waves (GWs) in General Relativity (GR)

Weak field:

$$g_{ab} = \eta_{ab} + h_{ab}, \qquad |h_{ab}| \ll 1$$

Using the harmonic coordinate condition:

$$\Box \bar{h}_{ab} = -\frac{16\pi G}{c^4} T_{ab} \qquad \left(\partial^a \bar{h}_{ab} = 0, \quad \bar{h}_{ab} = h_{ab} - \tfrac{1}{2}\eta_{ab} h\right)$$

In vacuum: homogeneous solution, plane waves with two polarisations

$$\Box \bar{h}_{ab} = 0 \quad \Rightarrow \quad \bar{h}_{ab} = \mathrm{Re}\left[\epsilon_{ab}\, e^{\,ik_c x^c}\right], \qquad k_c k^c = 0$$

Non-vacuum: inhomogeneous solution to the leading order:

$$h_{ij}^{\mathrm{TT}} \simeq \frac{2G}{c^4 r} \ddot{I}_{ij}^{\mathrm{TT}}\left(t - \frac{r}{c}\right), \qquad I_{ij} = \int \rho \left(x_i x_j - \tfrac{1}{3}\delta_{ij} x^2\right) \mathrm{d}^3 x$$

- The polarizations can be decomposed into spin-weighted spherical harmonics ${}_sY_{\ell m}$
- Higher harmonics appear beyond the leading order

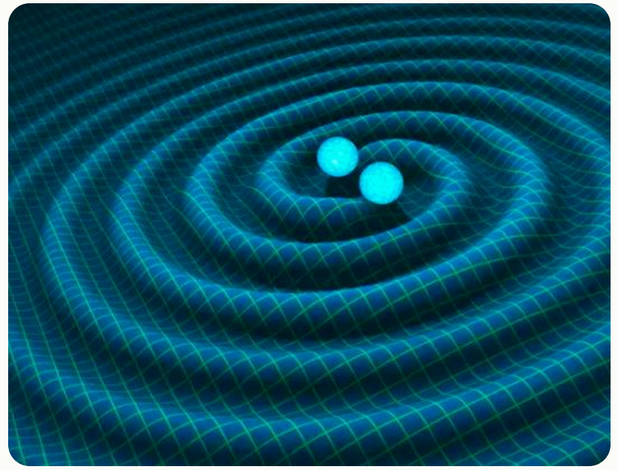
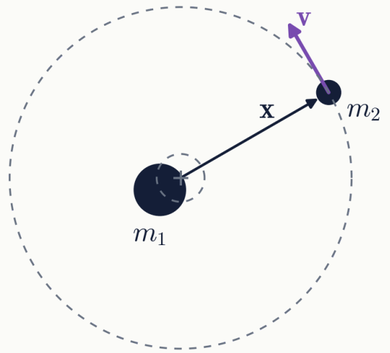


Illustration: R. Hurt / Caltech-JPL



Multipole expansion: Thorne, Rev. Mod. Phys. 52, 299 (1980); Blanchet, Living Rev. Relativ. 17, 2 (2014)

GR higher harmonics

$\delta = (m_1 - m_2)/M$

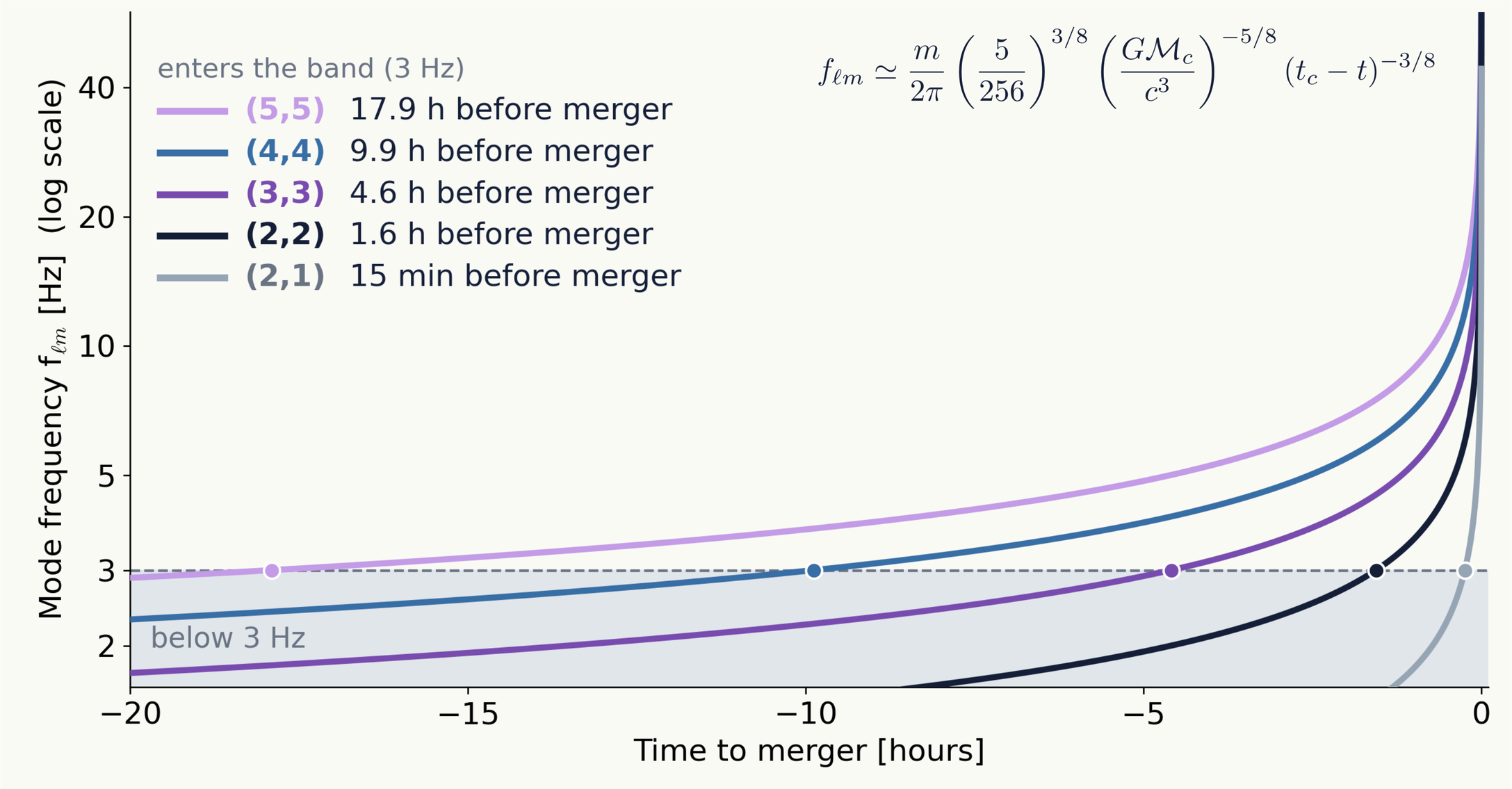
$\eta = m_1 m_2 / M^2$

v: orbital velocity in units of c

Mode (ℓ, m)	Radiated by	Frequency	Amplitude relative to (2,2)
(2,2)	mass quadrupole	2 × orbital	1
(2,1)	current quadrupole	1 × orbital	δ v
(3,3)	mass octupole	3 × orbital	δ v
(3,2)	current octupole	2 × orbital	$(1 - 3\eta)\ v^2$
(4,4)	mass hexadecapole	4 × orbital	$(1 - 3\eta)\ v^2$
(4,3)	current hexadecapole	3 × orbital	$\delta\ (1 - 2\eta)\ v^3$
(5,5)	mass $\ell = 5$ multipole	5 × orbital	$\delta\ (1 - 2\eta)\ v^3$

Leading-order amplitudes: Kidder, PRD 77, 044016 (2008); Blanchet, Living Rev. Relativ. 17, 2 (2014)

Peters, Phys. Rev. 136, B1224 (1964);
Maggiore, Gravitational Waves Vol. 1, OUP (2008), Ch. 4



NSBH 10 + 1.4 M⊙; curves: IMRPhenomXHM phase clock with f_ℓm = m f_orb

Which binaries emit higher harmonics?

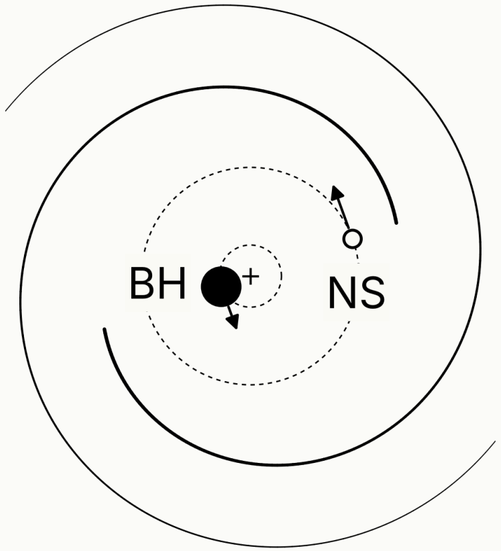
Loud when

the masses are unequal
the orbit is inclined, edge-on
late in the inspiral, fast orbits

Quiet when

the masses are equal: odd-m modes vanish
the orbit is face-on
early in the inspiral, slow orbits

Binary	Example masses	$\delta = (m_1 - m_2)/M$	Odd-m harmonics
NS + NS	1.4 + 1.4	0	vanish
NS + BH	e. g. 6 + 1.4 or 10 + 1.4	0.62 or 0.75	strong
BH + BH	e. g. 20 + 5 or 30 + 3	0.60 or 0.82	strong when unequal



NS + BH, schematic, not to scale
+ : centre of mass

Masses in M☉; NS + BH and BH + BH examples are the sources of this work

Higher harmonics have already been observed

GW190412

BH + BH

≈ 30 + 8 M⊙, q ≈ 0.28

strong evidence, $\log_{10} B \gtrsim 3$
strongest: (3,3)

Abbott et al., PRD 102, 043015 (2020)

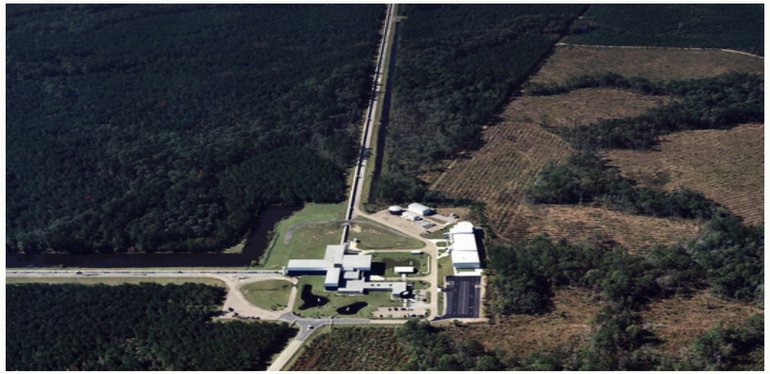
GW190814

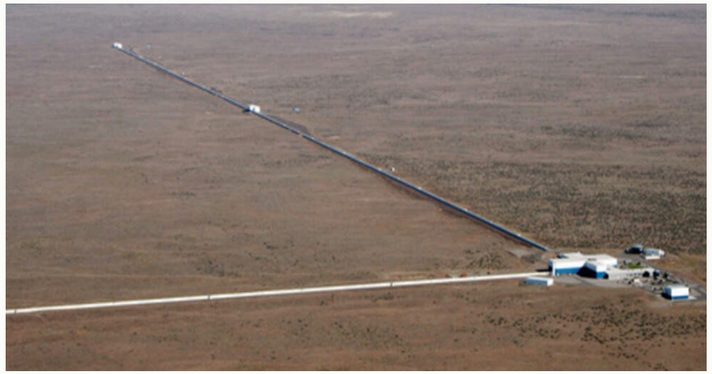
BH + NS ?

≈ 23 + 2.6 M⊙, q ≈ 0.11

very strong evidence, $\log_{10} B \approx 9.6$
strongest: (3,3), $\rho_{\perp} \approx 6.6$

Abbott et al., ApJL 896, L44 (2020)







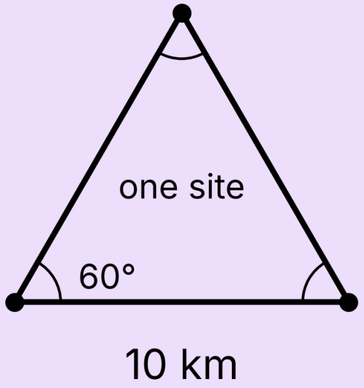
Photos: LIGO Livingston and LIGO Hanford, Caltech/MIT/LIGO Lab; Virgo, The Virgo Collaboration/CC0 1.0

The Einstein Telescope (ET)

- at least 10x more sensitive than 2nd gen. detectors
- lower frequency cutoff is around 3 Hz (LIGO-Virgo: 10-20 Hz)

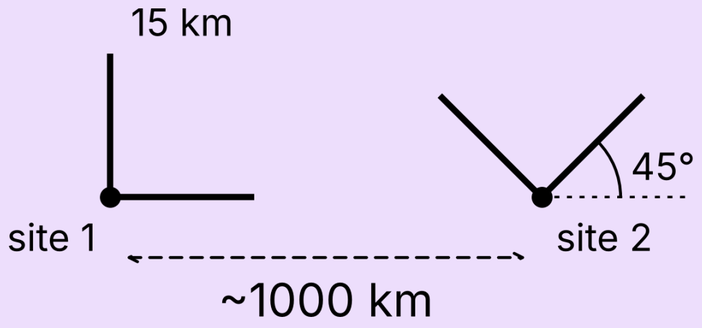
Triangle (10 km)

- one site
- three interferometers at 60°
- null stream: the sum of the three outputs cancels the signal



2L (15 km)

- two sites ~1000 km apart, arms at 45° to each other
- long baseline, better sky localisation



- Why 45°: complementary polarisation coverage
- aligned arms would favour the stochastic background (Branchesi et al. 2023).
- On a curved Earth, 45° is defined in each site's local frame (Bruno et al. 2026)

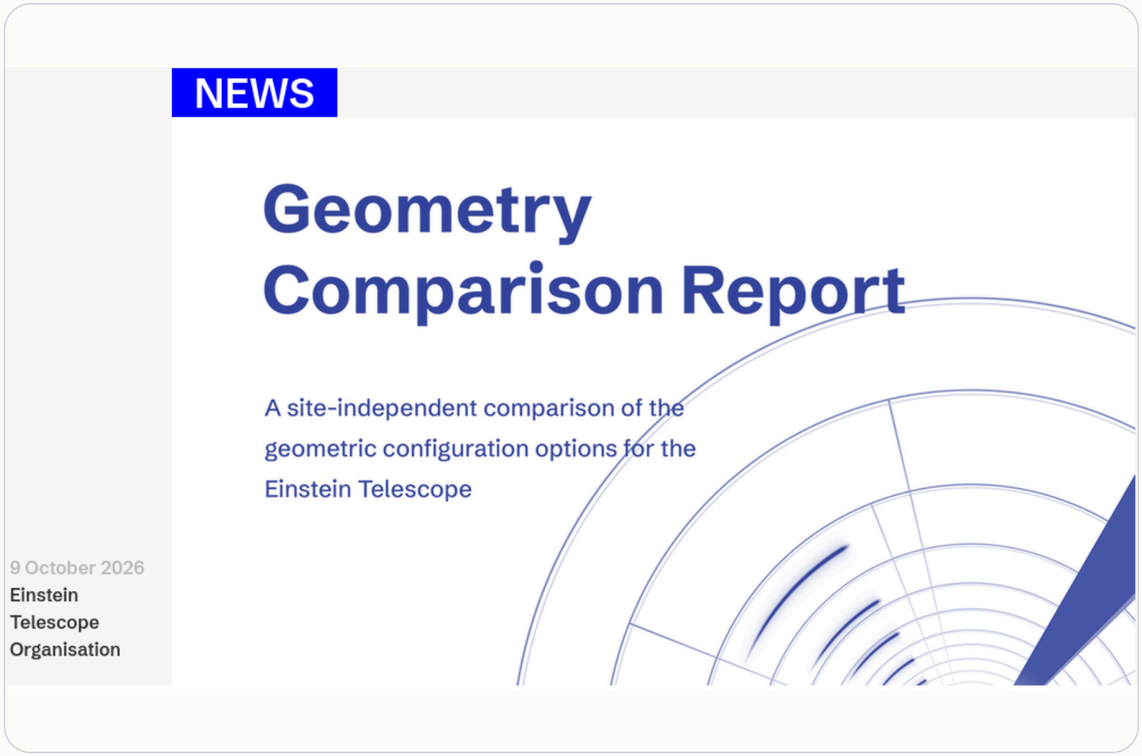
Three candidate sites, three layouts



Candidate site	Where
Euregio Meuse–Rhine	BE–NL–DE border
Sardinia	Sos Enattos, Italy
Lusatia	Saxony, Germany

Layout in this work	Design
EMR triangle	10 km, one site
Sardinia–EMR	2L, 15 km, 1168 km apart
Sardinia–Lusatia	2L, 15 km, 1259 km apart

Site coordinates: ET Organisation, Geometry Comparison Report (2026)



ET Organisation, Geometry Comparison Report (October 2026)

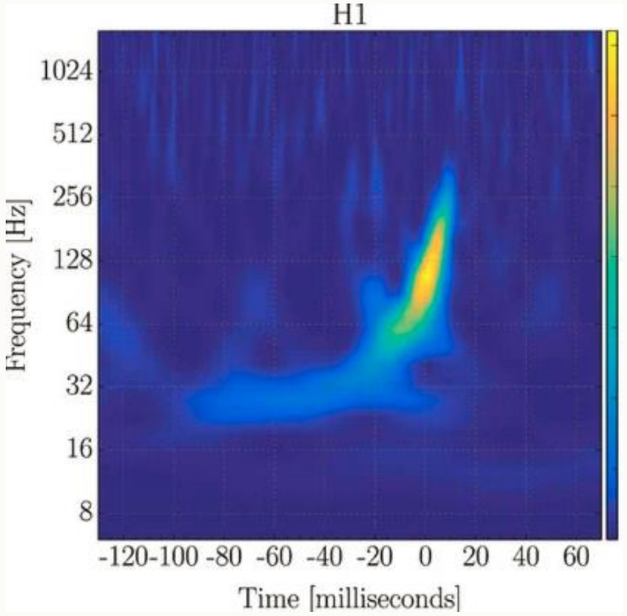
2021 ET on the ESFRI Roadmap

Jul 2026 Sardinia and Lusatia: joint 2L bid

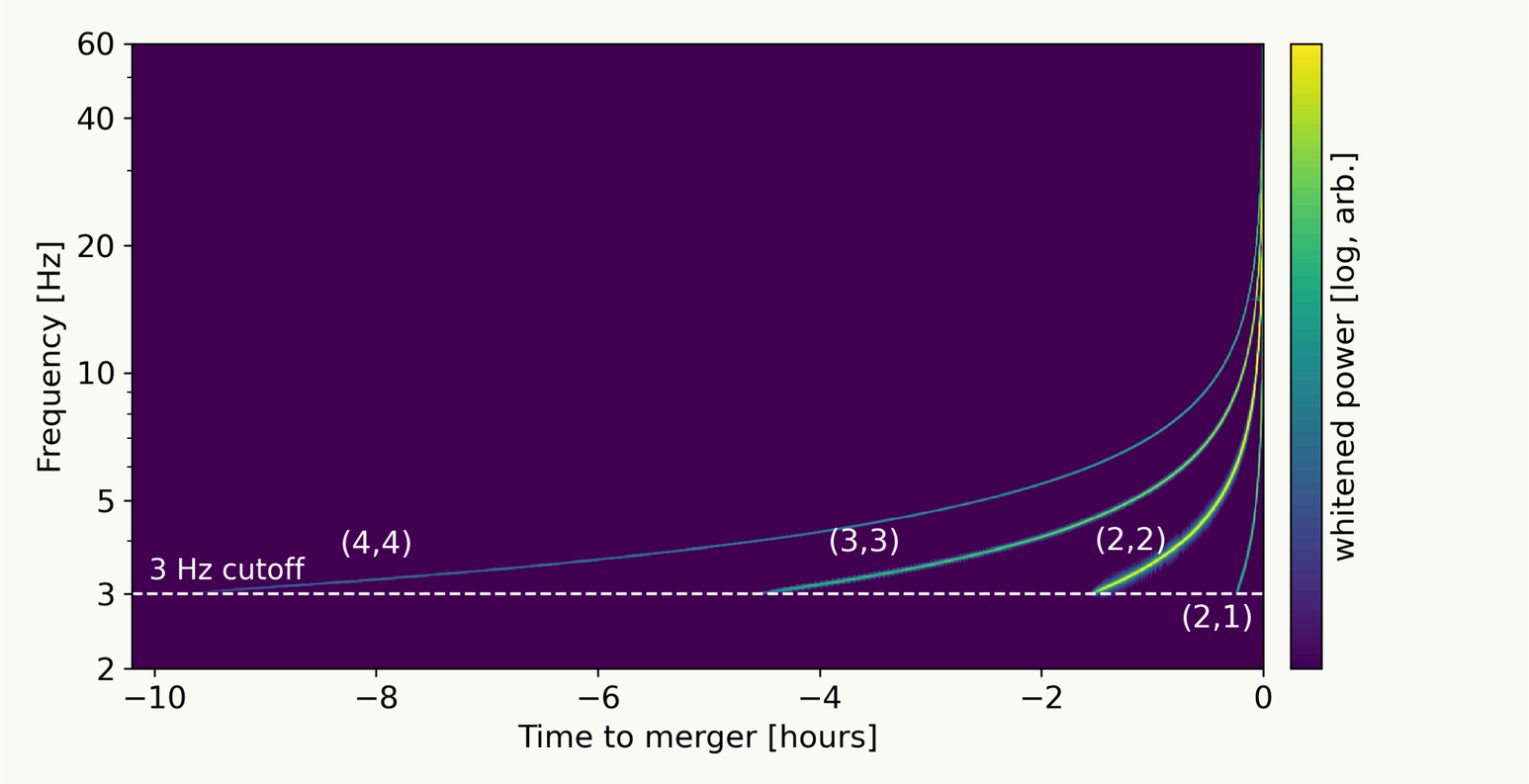
Oct 2026 Geometry Comparison Report: 10 km triangle vs. 15 km 2L

2027 site decision expected

What a signal looks like in ET



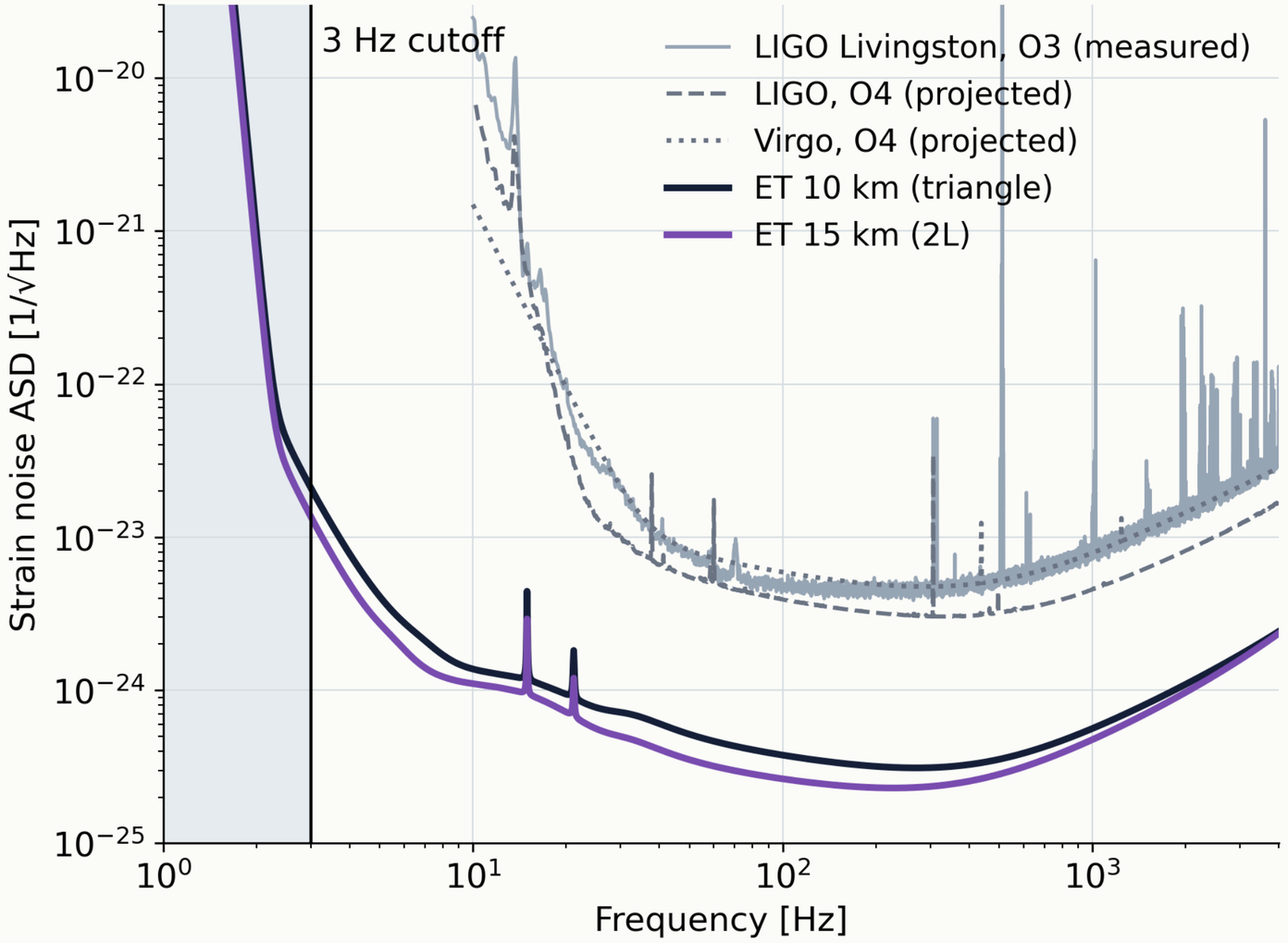
LIGO, GW150914: a fraction of a second



ET, simulated NSBH 10 + 1.4 M☉: hours

IMRPhenomXHM, 5 modes, inspiral only; 100 Mpc, ι = 60°; one Sardinia L, antenna pattern at merger; noise-free, whitened by the CoBA 15 km curve

GW150914: Abbott et al., PRL 116, 061102 (2016)



ET CoBA curves

10 km triangle

15 km L, the same at both sites

CoBA: the ET study comparing the candidate designs (triangle vs. 2L, 10–20 km arms); curves computed by the ET Instrument Science Board

Branchesi et al., JCAP 07, 068 (2023), arXiv:2303.15923
Data: Danilishin & Zhang, ET-0304B-22 (2023)

ET: Danilishin & Zhang, ET-0304B-22 (2023); LIGO/Virgo O4: LVK, Living Rev. Relativ. 23, 3 (2020); O3: LIGO-P2000251

The Earth rotates during the signal

$$h_I(t) = F_{+,I}(t)\, h_+(t) + F_{\times,I}(t)\, h_\times(t)$$

$$F_+ = \tfrac{1}{2}\left(1+\cos^2\theta\right)\cos 2\phi\,\cos 2\psi - \cos\theta\,\sin 2\phi\,\sin 2\psi$$

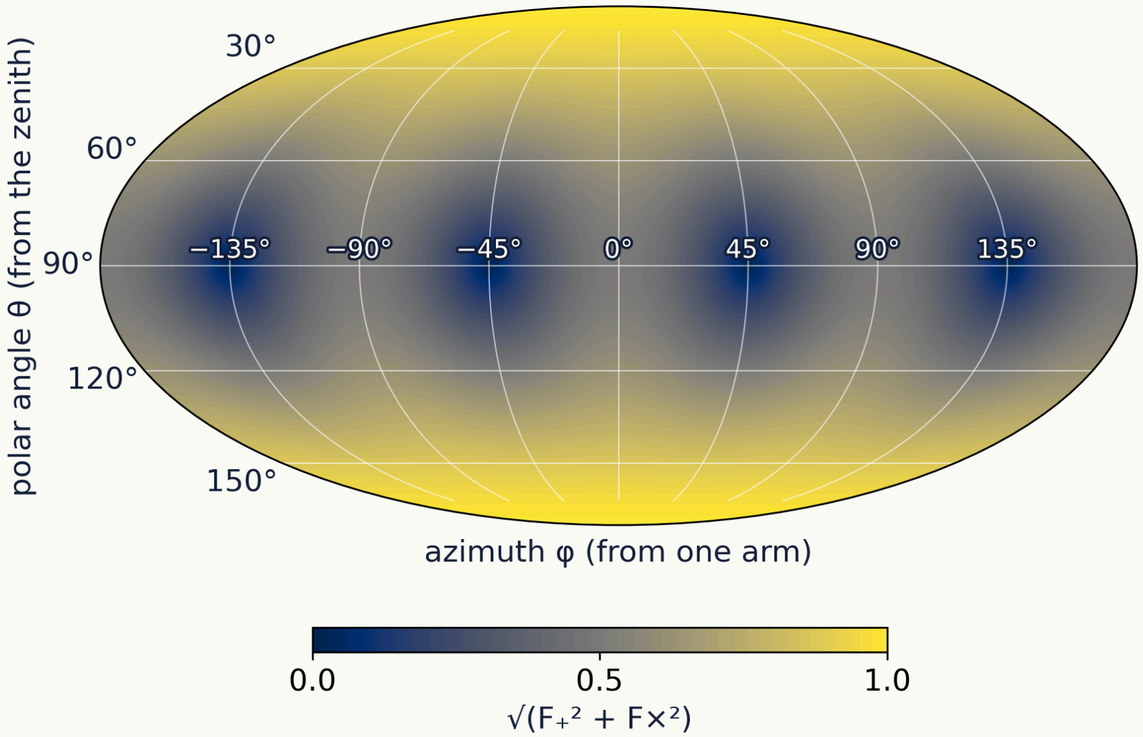
$$F_\times = \tfrac{1}{2}\left(1+\cos^2\theta\right)\cos 2\phi\,\sin 2\psi + \cos\theta\,\sin 2\phi\,\cos 2\psi$$

θ, φ: source direction in the detector frame (polar angle from the zenith, azimuth from one arm)
ψ: polarisation angle
60° arms (triangle): both multiplied by sin 60°

As the Earth rotates, θ and φ change: F_+ and $F\times$ depend on time.

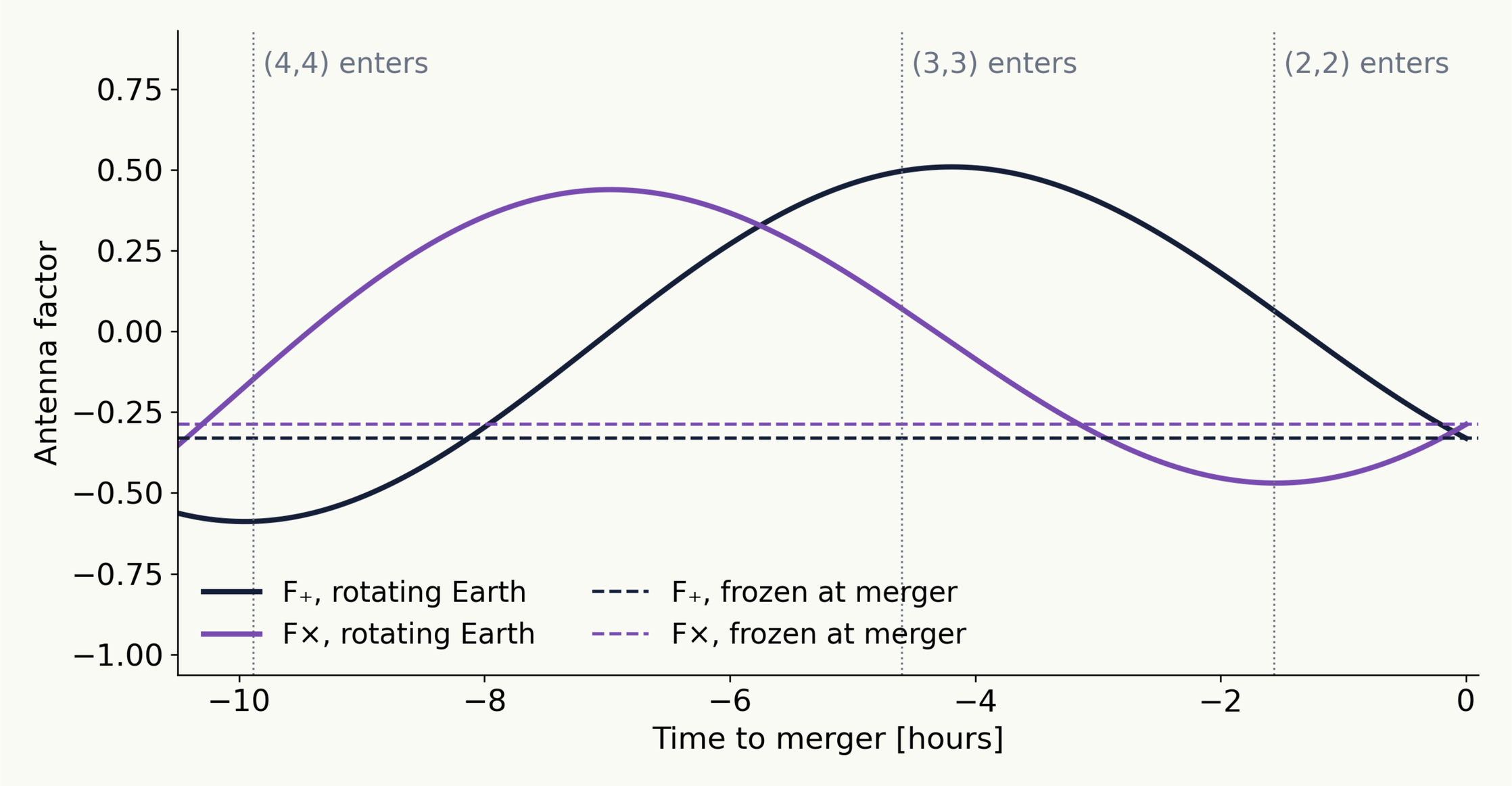
15° per hour

(a (4,4) mode in band for ~10 h sees ~150° of rotation)



Response of one L-shaped interferometer over the sky, detector frame (independent of ψ)

Antenna patterns: Sathyaprakash & Schutz, Living Rev. Relativ. 12, 2 (2009)



Sardinia L, principal sky position (α = δ = 60°, ψ = 12°); dashed: detector frozen at its merger orientation

Two waveform models used

IMRPhenomXHM

phenomenological, frequency domain

closed-form fits built on effective-one-body, post-Newtonian and numerical-relativity information

modes

(2,2) (2,1) (3,3) (3,2) (4,4)

García-Quirós et al., PRD 102, 064002 (2020)
LALSuite, doi:10.7935/GT1W-FZ16

SEOBNRv5HM

effective-one-body, time domain

the two-body motion mapped onto one body in an effective spacetime, calibrated to numerical relativity

modes

(2,2) (2,1) (3,3) (3,2) (4,4)
+ (4,3) (5,5)

Pompili et al., PRD 108, 124035 (2023)
pySEOBNR: Mihaylov et al., SoftwareX 30, 102080 (2025)

Shared modes compare the two models; (4,3) and (5,5) show what the extra modes add.

How much earlier does a mode enter?

Each mode oscillates at a multiple of the orbital frequency

$$f_{\ell m} \simeq m\, f_{\rm orb}$$

↓

ET hears it once it reaches 3 Hz: for larger m, at a lower orbital frequency

$$f_{\ell m} = f_{\rm low} \quad \Longleftrightarrow \quad f_{\rm orb} = \frac{f_{\rm low}}{m}$$

↓

A lower orbital frequency means more time left until merger (leading order):

$$t_c - t_m(f) = \frac{5}{256}\left(\frac{G\mathcal{M}_c}{c^3}\right)^{-5/3}\left(\frac{2\pi f}{m}\right)^{-8/3}$$

independent of distance, sky position and detector; shorter for heavier binaries

Divide by the same time for the (2,2): the masses cancel

$$\frac{\Delta t_m}{\Delta t_{22}} = \left(\frac{m}{2}\right)^{8/3}$$

Leading-order (Newtonian) chirp; the full-model entry clocks follow these ratios to within ~1–2 %

When does each mode enter the band?

Binary $m_1 + m_2$ [$M_\odot$]	Band entry at 3 Hz: time before merger [min]				
	(2,1)	(2,2)	(3,3)	(4,4)	(5,5)
NSBH 6 + 1.4	21	135 2.3 h	397 6.6 h	855 14.2 h	1549 25.8 h
NSBH 10 + 1.4	15	94 1.6 h	276 4.6 h	593 9.9 h	1074 17.9 h
BBH 20 + 5	2.7	17	50	108 1.8 h	196 3.3 h
BBH 30 + 3	3.2	21	61 1.0 h	132 2.2 h	239 4.0 h

Zero spins; ι = 60° in all results that follow (entry times do not depend on it); hours given below each entry. (5,5): the time when the orbital frequency reaches 0.6 Hz, from the IMRPhenomXHM phase clock; for NSBH 10 + 1.4 it agrees with the SEOBNRv5HM (5,5) clock to 0.01 s.

How loud are the higher harmonics?

$$\rho^2 = 4\int_{f_{\mathrm{low}}}^{f_{\mathrm{max}}} \frac{|\tilde{h}(f)|^2}{S_n(f)}\,\mathrm{d}f$$

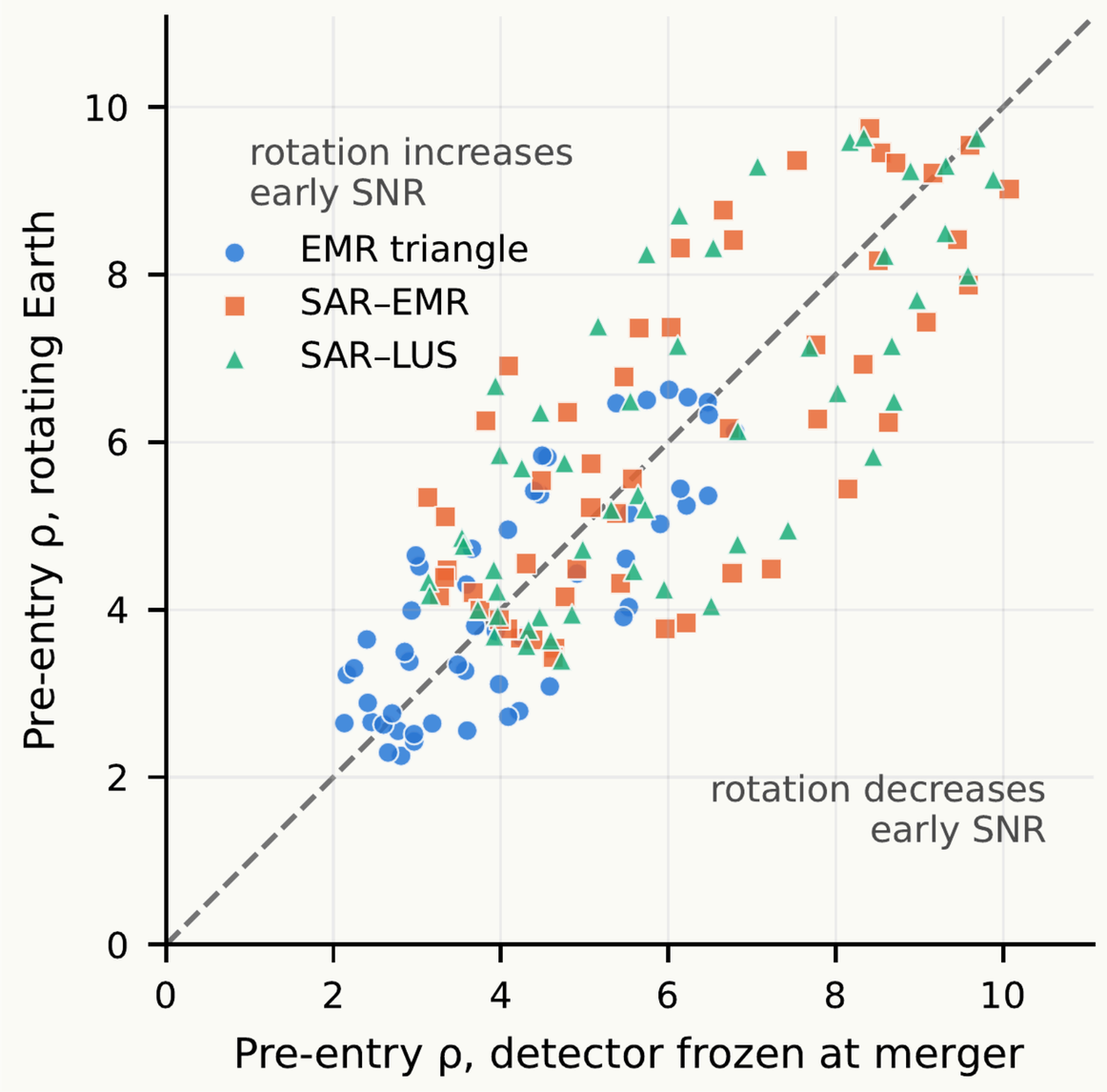
ħ(f): the signal

$S_n(f)$: the detector noise

Matched filtering: comparing the data with a known waveform

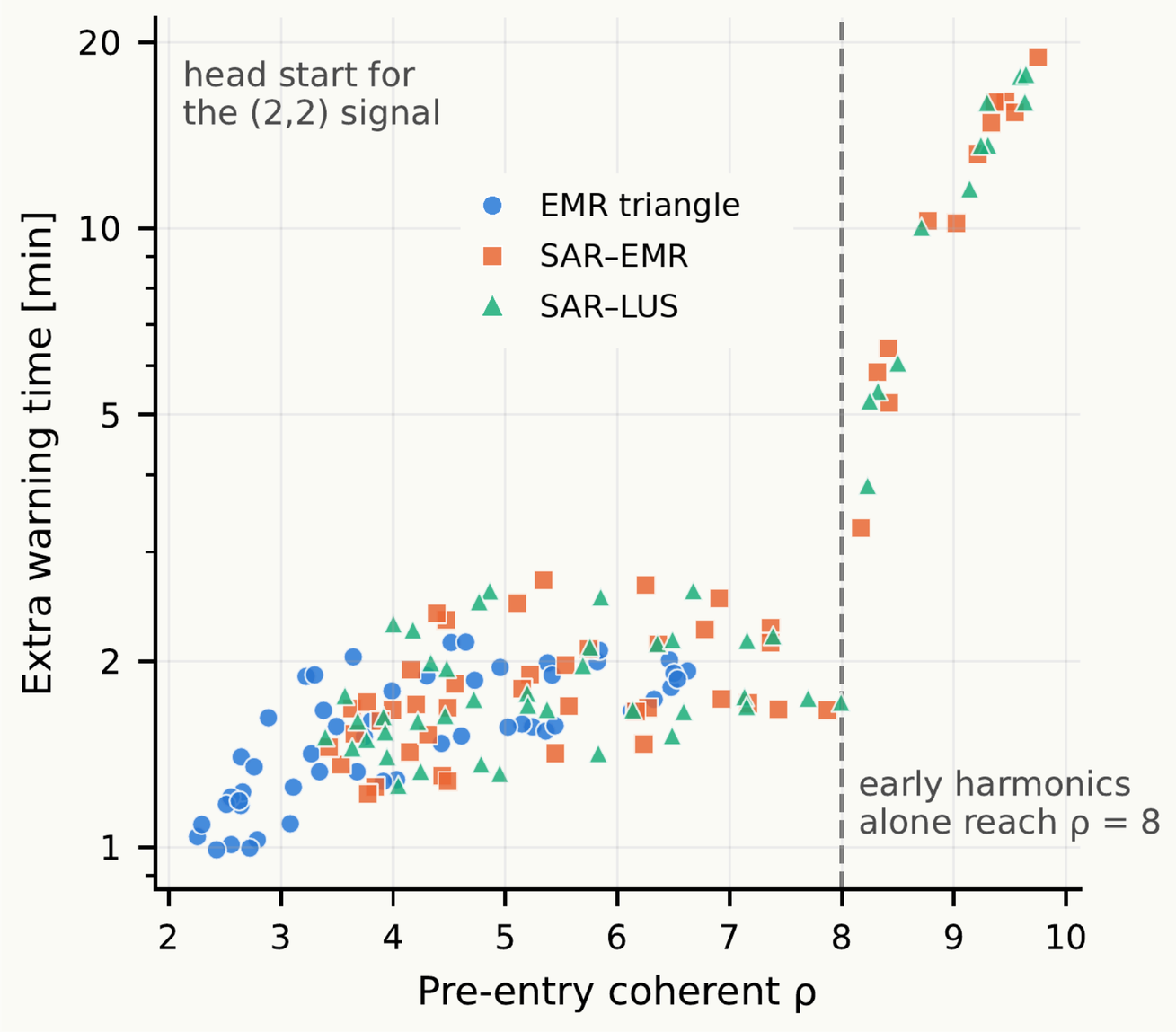
- **ρ* ≈ 8–10**: detection threshold
- **alert time**: when the accumulated ρ first crosses ρ*
- **pre-entry ρ**: collected before the (2,2) enters the band
- **ρ⊥**: the part of a mode the (2,2) cannot mimic; ρ⊥ = 2.1 is evidence, 5.3 is a confident detection

ρ⊥: Mills & Fairhurst, PRD 103, 024042 (2021)



- 52 combinations of sky position and arrival time (3 layouts)
- Earth's rotation influences the SNR values
- SNR may decrease by 38% or increase by 71%, important for a single event
- the median is 0.98 (cancels out), doesn't bias the population
- the 2L pairs are more sensitive than the EMR triangle

NSBH 10 + 1.4 M☉, 100 Mpc, ι = 60°



- early higher harmonics' entry provides a warning time
- The alert is when the accumulated network SNR crosses ρ ≈ 8
- ρ < 8: the early harmonics are not enough to trigger, still contribute 1-3 mins
- ρ ≥ 8: early harmonics trigger before the (2,2) enters, gain jumps to 19 mins
- only the 2L pairs reach the ρ ≥ 8 regime

NSBH 10 + 1.4 M☉, ι = 60°, ρ* = 8; 52 cases at 100 Mpc

The gain depends strongly on the source

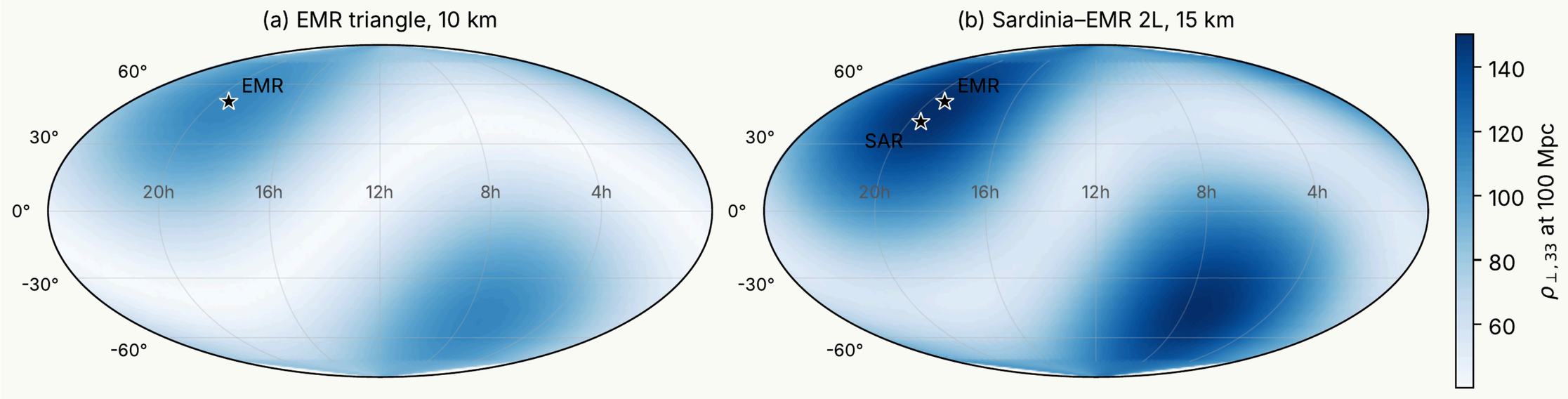
Binary	(2,2) enters [min]	Median extra warning [min]		
		Triangle	SAR–EMR	SAR–LUS
NSBH 6 + 1.4	135	0.8	1.1	1.1
NSBH 10 + 1.4	94	1.4	1.7	1.7
BBH 20 + 5	17	0.4	5.1	5.4
BBH 30 + 3	21	**4.6**	**12.7**	**13.1**

100 Mpc, medians over 52 sky/time cases

The 2L pairs see all modes better: in every row they give more warning than the triangle.

Heavy, asymmetric binaries: the (2,2) arrives late and the harmonics are loud. The gain drops quickly with distance.

ρ* = 10; masses in solar masses; ι = 60°, zero latency; (2,2) enters: minutes before merger



×1.3 2L / triangle SNR, every mode (median)

×1.02 2L / triangle higher-mode fraction

includes 15 km vs. 10 km arms and noise curves

Map: (3,3) orthogonal SNR, NSBH 10 + 1.4 M☉, ι = 60°, 100 Mpc, polarisation-averaged

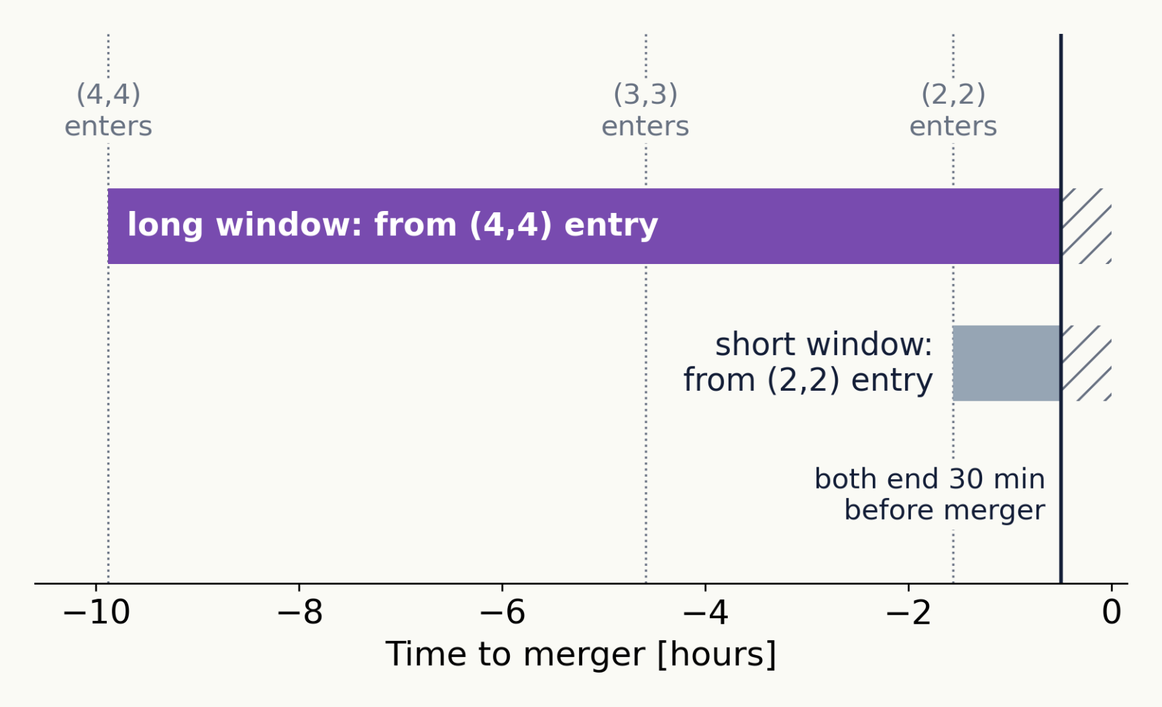
Do higher harmonics improve source characterization?

- Hypothesis: early harmonics improve precision of parameter estimation (PE)
- The more a parameter influences the signal, the more precise its measurement
- Inclination - distance degeneracy may be resolved

  Step 1: preliminary Fisher calculation

  Step 2: conditional Bayesian PE

  Step 3: full Bayesian PE with all parameters free



Compare the two windows: the only difference is the early higher-harmonic data

NSBH 10 + 1.4 M☉, 100 Mpc, ι = 60°, principal sky position; IMRPhenomXHM, rotating Earth

Step 1: Fisher calculation

Full Fisher (10 parameters)

$$(\ln \mathcal{M}_c,\ \eta,\ \chi_1,\ t_c,\ \phi_c,\ \ln D,\ \iota,\ \alpha,\ \delta,\ \psi)$$

chirp mass, symmetric mass ratio, BH spin, merger time and phase, distance, inclination, two sky coordinates and polarisation (NS spin fixed)

With a waveform $h(\boldsymbol{\theta})$, where $\boldsymbol{\theta}$ are the parameters:

A derivative such as $\dfrac{\partial h}{\partial \iota}$ describes how the predicted signal changes when inclination changes slightly.

The Fisher matrix is $\Gamma_{ij} = \left(\dfrac{\partial h}{\partial \theta_i} \middle| \dfrac{\partial h}{\partial \theta_j} \right)$

We assume loud signals with a nearly Gaussian likelihood: $C \simeq \Gamma^{-1}, \qquad \sigma_i \simeq \sqrt{C_{ii}}$

In a Gaussian, the matrix in the exponent is the inverse covariance.

Linearity test (Vallisneri 2008)

We assume linear changes in the waveform.

$$h(\boldsymbol{\theta} + \Delta\boldsymbol{\theta}) \simeq h(\boldsymbol{\theta}) + \sum_i \partial_i h\, \Delta\theta_i$$

In the early inspiral, masses and spins can partly compensate for each other's effects on the phase.

Linearity test: Vallisneri, PRD 77, 042001 (2008). ET Fisher forecasts: GWFAST, Iacovelli et al., ApJS 263, 2 (2022)
Fisher checked by full PE on selected events: Iacovelli et al., PRD 108, 122006 (2023)

Step 1: Conditional Fisher calculation

Masses, spin, time and phase fixed; free: $(\ln D,\ \iota,\ \alpha,\ \delta,\ \psi)$ distance, inclination, two sky coordinates and polarisation

- “Conditional” means: we fix certain parameters
- Fixing parameters prevents them from compensating for changes in the free ones

long → short	σ(ln D)	σ(ι)	sky 90 % [deg²]
Triangle	0.27 → 0.30	7.4° → 8.4°	137 → 155
SAR–EMR	0.19 → 0.22	5.9° → 6.6°	53 → 60
SAR–LUS	0.18 → 0.21	5.3° → 6.0°	45 → 51

- arrows run long → short: the uncertainties grow when the early data are discarded
- σ(ln D) = 0.27 ≈ 27 % fractional distance uncertainty, not 0.27 Mpc

Result: a modest, consistent improvement, ≈ 10 %, varying with source position and observing time (7–12 % over 4 sky/time cases)

NSBH 10 + 1.4 M☉, 100 Mpc, ι = 60°, principal sky position; both windows end 30 min before merger

Step 2: Conditional Bayesian PE

Fixed: masses, spins, merger time
Sampled: distance, inclination, sky position, polarisation and now also the phase

Instead of one Gaussian near the peak, we evaluate the posterior:

$$p(\boldsymbol{\theta} \mid d) \;\propto\; p(d \mid \boldsymbol{\theta})\,\pi(\boldsymbol{\theta})$$

- likelihood $p(d|\boldsymbol{\theta})$: agreement between a candidate waveform and the data
- prior $\pi(\boldsymbol{\theta})$: parameter distribution assumed before analysing the data

Sampling captures asymmetric distributions, can show bimodality

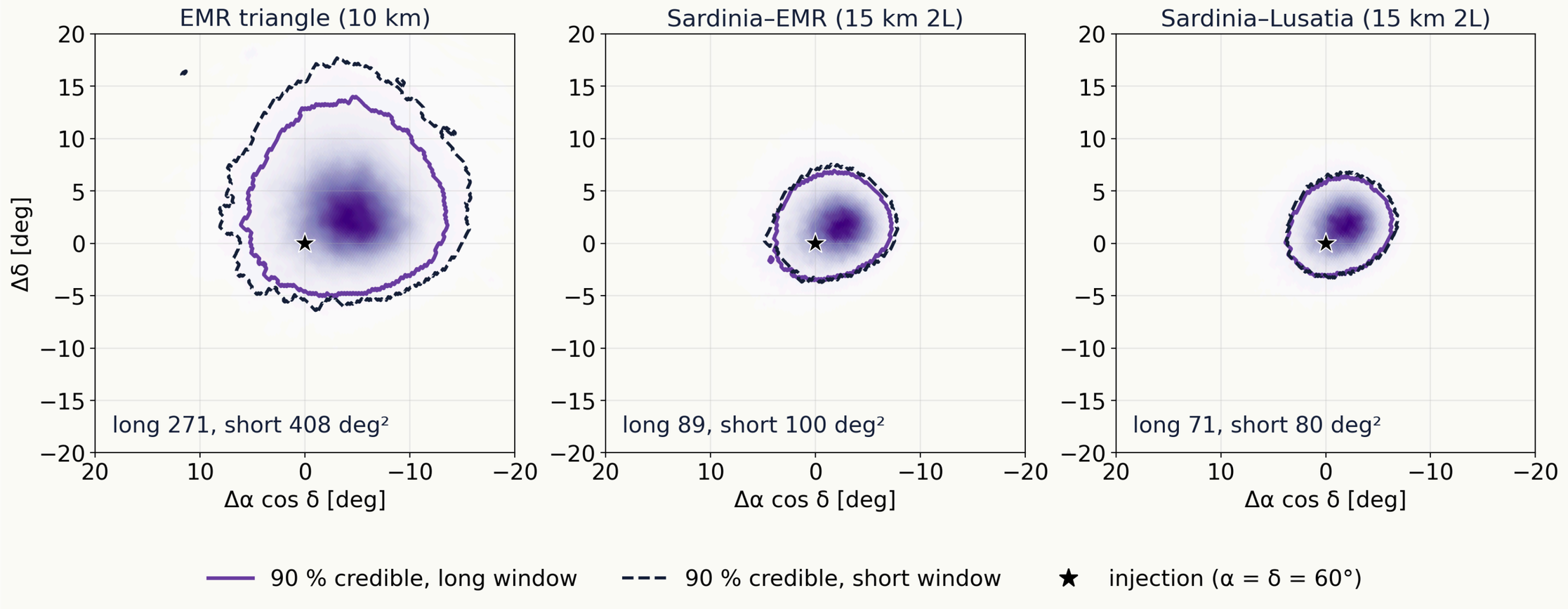
We assumed Gaussian detector noise in the likelihood, using the ET noise curves

Configuration	long	short	early data
EMR triangle	271	408	−34 %
SAR–EMR	89	100	−11 %
SAR–LUS	71	80	−10 %

90 % credible sky area [deg²], principal source

- the early-data improvement survives posterior sampling; distance and inclination intervals ≈ 2–8 % narrower
- the triangle gains most, but remains the poorer localiser: 2L areas are 3.1–3.8× smaller (long), 4.1–5.1× (short)

Conditional posteriors, importance sampling; NSBH 10 + 1.4 M☉, 100 Mpc, ι = 60°; windows end 30 min before merger



Posterior sky maps, zoomed on the injected position (principal source); 40° × 40° around α = δ = 60°

Step 3: Full Bayesian PE (ongoing)

- All parameters free; currently ongoing with the IMRPhenomXHM waveform model.
  - 23–24% narrower chirp-mass uncertainties (long vs. short window).
  - 28–33% narrower effective-spin uncertainties (long vs. short window).
- Planned full Bayesian PE run for uncovering bias between waveform models
  - Inject SEOBNRv5HM signals and analyse them with IMRPhenomXHM

Waveform models: IMRPhenomXHM and SEOBNRv5HM (see slide 14)

Thank you for your attention!

karacsonyi.kata@wigner.hu

Image: R. Hurt / Caltech-JPL

From the source to the quadrupole formula

1 Solve the inhomogeneous wave equation with the retarded Green's function

$$\bar{h}_{ab}(t,\mathbf{x}) = \frac{4G}{c^4}\int \frac{T_{ab}(t-|\mathbf{x}-\mathbf{x}'|/c,\ \mathbf{x}')}{|\mathbf{x}-\mathbf{x}'|}\,\mathrm{d}^3x'$$

2 Far from the source ($r \gg$ its size) and slow motion ($v \ll c$): $|x - x'| \approx r$

$$\bar{h}_{ij}(t,\mathbf{x}) \simeq \frac{4G}{c^4\,r}\int T_{ij}\left(t-\frac{r}{c},\,\mathbf{x}'\right)\mathrm{d}^3x'$$

3 Energy–momentum conservation ($\partial_a T^{ab} = 0$) turns the stresses into the mass distribution

$$\int T^{ij}\,\mathrm{d}^3x = \frac{1}{2}\frac{\mathrm{d}^2}{\mathrm{d}t^2}\int \frac{T^{00}}{c^2}\,x^i x^j\,\mathrm{d}^3x = \frac{1}{2}\,\ddot{I}^{ij}, \qquad T^{00} \simeq \rho c^2$$

4 Keep the transverse-traceless (TT) part, the only part that radiates

$$h_{ij}^{\mathrm{TT}} \simeq \frac{2G}{c^4\,r}\,\ddot{I}_{ij}^{\mathrm{TT}}\left(t-\frac{r}{c}\right)$$

The trace of I_{ij} drops out in the TT projection, so I_{ij} can be taken trace-free (the reduced quadrupole).

See e.g. M. Maggiore, Gravitational Waves, Vol. 1 (Oxford University Press, 2008), Ch. 3